The influence of hole dimensions on static pressure measurements

By R. SHAW
Department of Mechanical Engineering, University of Liverpool

(Received 1 July 1959)

The pressure measured at a static pressure hole differs slightly from the true static pressure, by an amount which depends on the hole size and shape. The present investigation extends the range of previous work to determine the error in static pressure measurement in incompressible turbulent flow. The observed static pressure was always greater than the true static pressure. The results are presented in dimensionless form as a function of the Reynolds number based on hole diameter and friction velocity.

1. Introduction

Previous investigations have shown that the observed static pressure is influenced by the dimensions of the static pressure hole. The flow near to the wall is disturbed by the hole, and the fluid in the hole is set in motion by the fluid passing it. An infinitely small hole has been assumed to give the correct reading, and the experimental results for relative errors have been extrapolated to zero hole diameter in order to assess the absolute error.

Investigations have been carried out by Fuhrmann (1912), Allen & Hooper (1932), Myadzu (1936), and Ray (1956) for incompressible flow and by Rayle (1949) for both incompressible and compressible flow. Ray correlated his results by employing the principle of dimensional similarity and expressed the error as a function of the Reynolds number and the length/diameter ratio of the hole. Rayle correlated his results on a Mach number basis. The present experiments extend the range of results for incompressible turbulent flow.

Fuhrmann employed a model in a wind tunnel in which the air velocity was 32 ft./sec. The model consisted of a body of revolution with very thin walls and three interior compartments. A 0·031 in. diameter hole located in the wall of the centre compartment served as a reference, while two test holes located diametrically opposite at the front compartment were varied in size from 0·005 in. diameter to 0·043 in. diameter. For sharp-edged holes, negative errors were observed. These errors increased rapidly with increase of hole size up to 0·016 in. diameter, the error then becoming nearly constant.

Allen & Hooper experimented with a 12 in. diameter pipe which had been cleaned by scraping. The static pressure holes were located in $\frac{3}{4}$ in. diameter removable plugs which were scraped flush with the bore of the pipe. The experiments were carried out with water flowing at velocities from 4 to 7·3 ft./sec. For holes varying in diameter from $\frac{1}{16}$ to $\frac{27}{32}$ in. no error was recorded. An $\frac{1}{8}$ in. radius

on an $\frac{1}{8}$ in. diameter hole gave a positive error, but smaller radii ($\frac{1}{16}$ and $\frac{1}{32}$ in.) gave the same reading as a sharp-edged hole and were therefore recommended in order to ensure freedom from burrs.

Myadzu employed a channel of square section with water flowing at velocities up to 14 ft./sec. Adjustable plugs with static pressure holes varying from 0·004 to 0·157 in. diameter were used to obtain the error relative to a line of reference holes equally spaced along the channel length to record the fall in pressure. The absolute error was found by graphical extrapolation, and the results indicated a positive error which increased linearly with hole size but was independent of velocity. The depth of hole was significant; the error was constant for length/diameter ratios greater than 2, but decreased for smaller ratios, until below a ratio of about 0·4 negative errors were indicated.

Rayle located a 1 in. diameter test section at various distances downstream of a nozzle, and used insert plugs with static pressure holes of length/diameter ratio greater than 2·5 and diameter varying from 0·006 to 0·125 in. Both air at mean velocities from 400 to 900 ft./sec and water at velocities from 22 to 31 ft./sec were employed in order to observe the effects of compressibility. Positive errors were recorded, and these errors were found to increase with increase in hole diameter, with increase of Mach number and with reduction of the distance between the nozzle and test section. Various edge forms were tested for 0·032 and 0·046 in. diameter holes. A radius was found to increase the positive error, whilst a chamfer produced a negative change.

Ray's experiments were carried out using a sugar solution, the concentration of which was varied to give kinematic viscosities between 0·01 and 0·03 ft.^{2}/sec. Velocities up to 12 ft./sec were employed. The test section was rectangular, measuring 2·8 × 1·6 in., with static pressure holes located in the longer lower side. The diameter of the holes was varied from 0·039 to 0·393 in., and the length/diameter ratio from 1·75 down to 0·1. The diameter of the connexion to the manometer was also varied, being smaller than the hole diameter for most of the tests. The results indicated that the error was positive and increased with increase of the Reynolds number and reduction of the length/diameter ratio. Ray's results expressed in similar form to that used in the present report give

$$\frac{\Delta P}{\tau_0} = \frac{C}{2}\left\{\frac{d}{\nu}\sqrt{\frac{\tau_0}{\rho}}\right\}^{\frac{1}{2}},$$

where ΔP is the absolute static pressure error, τ_0 the wall shear stress, l the length of the hole of diameter d, ν the kinematic viscosity, and ρ the density. Here $C = f\{l/d\}$ varies from 0·5 when $l/d = 1{\cdot}75$ to 1·08 when $l/d = 0{\cdot}1$. His results cover the range $1{\cdot}7 < R < 31{\cdot}6$, where $R = (d/\nu)\sqrt{(\tau_0/\rho)}$ is the Reynolds number based on hole diameter and friction velocity. Negative pressure errors were recorded only when the length/diameter ratio was very small and the enlargement behind the hole considerable.

Thom & Apelt (1957) have calculated the pressure in a two-dimensional static hole at low Reynolds numbers, by means of an arithmetical method for the solution of the Navier–Stokes equations. The solution is for laminar flow and is valid for the Reynolds numbers $u_1 w/\nu$ up to 1, where u_1 is the velocity at the

centre line and w the width of a two-dimensional static hole. It is suggested that there might be two different functions for the dimensionless pressure error, one for laminar flow and one for turbulent flow, connected by a range of transition values, as in the case of resistance to flow in a pipe. The solution is modified to give the dimensionless pressure error for the three-dimensional case of a circular hole. If Nikuradse's results for the resistance to flow in pipes are extrapolated to very small Reynolds numbers, this solution can be expressed in similar form to that used in the present report. At the upper limit ($u_1 w/\nu = 1$) for which the solution is valid, $\Delta P/\tau_0 = 0{\cdot}088$ and $(d/\nu)\sqrt{(\tau_0/\rho)} = 1{\cdot}4$.

2. True static pressure

The flow behaviour at the static pressure hole is shown in figure 1. The deflexion of the streamline into the hole is confirmed by the analysis for a two-dimensional hole by Thom & Apelt (1957). The curvature of the streamline is such as to increase the static pressure in the hole above the true value for the pipe. There is also an eddy or system of eddies set up in the hole and a Pitot effect at the downstream edge of the hole. These three factors combine to give the net pressure error. For a fixed speed of flow it is probable that these effects will decrease as the hole size decreases, so that $\Delta P \to 0$ as $d \to 0$.

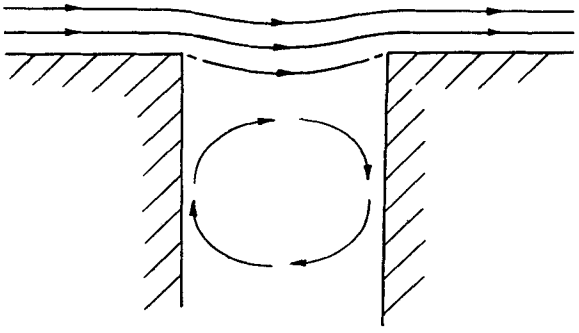

FIGURE 1. Flow behaviour at the static pressure hole.

3. Local dynamical similarity considerations

We assume initially that the static hole is small compared with the diameter of the pipe (or thickness of the boundary layer on a plate), that the geometry of the hole and manometer connexion remains similar, and that the pipe surface is smooth. Under these circumstances the pressure error for a finite hole size can be influenced only by the hole diameter d, the fluid density ρ, the absolute viscosity μ, and the local flow conditions at the surface. Now for a distance y up to approximately one-fifth of the pipe radius or boundary-layer thickness from the wall, the local velocity u is given by

$$\frac{u}{\sqrt{(\tau_0/\rho)}} = f\left\{\frac{y}{\nu}\sqrt{\frac{\tau_0}{\rho}}\right\},$$

from which it is apparent that u at distance y from the wall depends on τ_0, ρ and μ. It is therefore the velocity gradient, described by the wall shear stress τ_0, which defines the local flow conditions.

Since for a very small hole the fluid is not disturbed by the hole, it may be assumed that as d tends to zero the measured pressure tends to the true static pressure. (See next section where this is discussed further.) Accounting for the variables suggested above, the static pressure error for a finite hole size can therefore be written

$$\Delta P = f\{\tau_0, \rho, \mu, d\},$$

or

$$\frac{\Delta P}{\tau_0} = f\left\{\frac{d}{\nu}\sqrt{\frac{\tau_0}{\rho}}\right\}. \tag{1}$$

Allowing for changing hole and connexion geometry and increase of hole diameter until the hole-diameter/pipe-diameter ratio is significant, equation (1) can be rewritten

$$\frac{\Delta P}{\tau_0} = f\left\{\frac{d}{\nu}\sqrt{\frac{\tau_0}{\rho}}, \frac{l}{d}, \frac{D}{d}, \frac{D_p}{d}\right\}, \tag{2}$$

where D is the diameter of the connexion to the manometer and D_p the diameter of pipe.

4. Behaviour of $\Delta P/\tau_0$ as $(d/\nu)\sqrt{(\tau_0/\rho)} \to 0$

It is impossible to experiment with extremely small holes or with very small velocities, so that $(d/\nu)\sqrt{(\tau_0/\rho)}$ cannot be reduced to indefinitely small values. It is therefore impossible to establish the true static pressure directly, and extrapolation is necessary. This procedure could lead to inaccuracies unless there is some theoretical guide to the behaviour of the error as $(d/\nu)\sqrt{(\tau_0/\rho)} \to 0$.

For any given fluid (density ρ and absolute viscosity μ fixed) the friction velocity $\sqrt{(\tau_0/\rho)}$ falls as the flow velocity is reduced, and the region in which the viscous stresses are important increases in thickness. Close to the surface the viscous stresses are large compared with the dynamic stresses, since the velocity $u \to 0$. The effect of density on the motion is therefore negligible, and it can therefore be eliminated from the variables involved. Thus $\Delta P = f\{\tau_0, \mu, d\}$. Only one dimensionless group can be formed, so that

$$\Delta P/\tau_0 = \text{const.} \tag{3}$$

Since it is inferred that $\Delta P/\tau_0 \to 0$ as $d \to 0$, equation (1) shows that $\Delta P/\tau_0$ must also approach zero as $(d/\nu)\sqrt{(\tau_0/\rho)} \to 0$. Thus the constant in equation (3) must be zero, and therefore $\Delta P/\tau_0 \doteq 0$ as $(d/\nu)\sqrt{(\tau_0/\rho)}$ becomes small.

5. Behaviour of $\Delta P/\tau_0$ when $(d/\nu)\sqrt{(\tau_0/\rho)}$ is large

For a pipe of large diameter (or very thick boundary layer on a plate), increasing the static hole diameter for a fixed velocity will result in a greater flow into and out of the hole and the turbulent velocity component v' will no longer vanish at the hole position. Thus, for large holes, turbulent stresses may outweigh the viscous stresses. Also the Pitot effect at the downstream edge of the hole, which is a dynamic effect, will outweigh the viscous effects. Hence the viscosity may now be eliminated from the variables. Thus $\Delta P = f\{\tau_0, \rho, d\}$, and $\Delta P/\tau_0 = \text{const.}$ as only one dimensionless group can be formed. Thus the curve of $\Delta P/\tau_0$ *vs* $(d/\nu)\sqrt{(\tau_0/\rho)}$ must be as shown in figure 2.

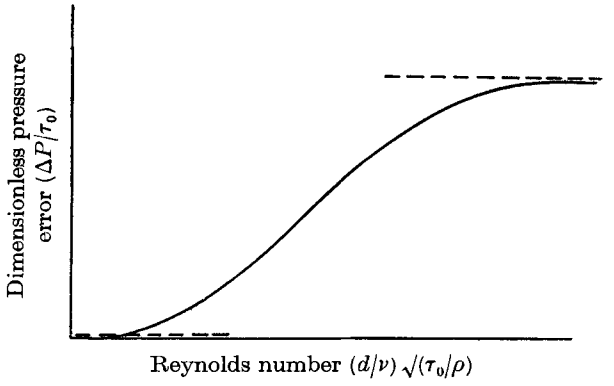

FIGURE 2. Predicted curve of dimensionless pressure error against Reynolds number.

6. Apparatus

The general assembly of the apparatus is shown in figure 3. Air was drawn through 30 ft. of 2 in. internal diameter brass pipe by either a three-stage centrifugal blower or a small single-stage blower, and the air flow was measured by a $\frac{3}{4}$-radius Pitot tube flow meter (Preston 1950). The pipe inlet was shaped to reduce losses and was followed by a transition ring to promote turbulence (Preston 1958).

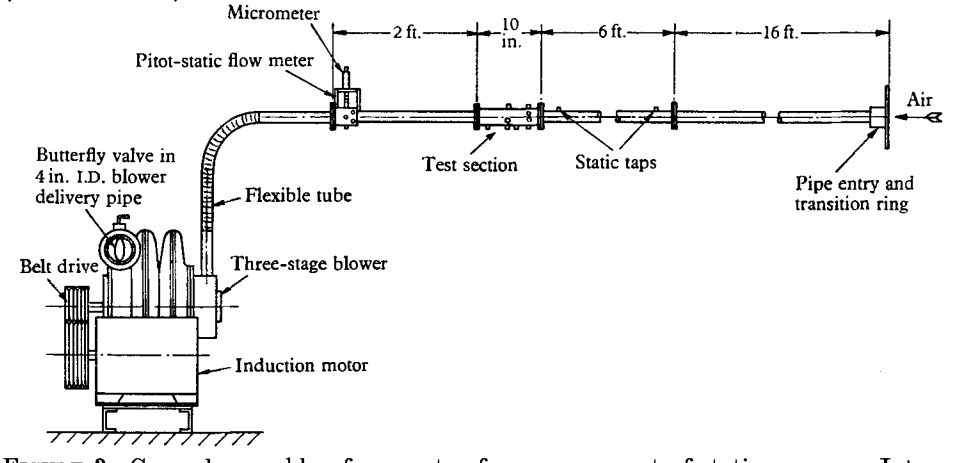

FIGURE 3. General assembly of apparatus for measurement of static pressure. Internal diameter of pipe = 2 in.; mean flow velocity 38–212 ft./sec.; all pipe joints carefully blended and flanges dowelled for accurate location.

The test section shown in figure 4 was located at 130 diameters from the inlet, in a region of fully developed turbulent flow. It consisted of a 10 in. long 2 in. internal diameter pipe made from $2\frac{3}{4}$ in. diameter solid brass, split on a diameter to facilitate inspection of the static pressure holes. The test section and the immediate upstream pipe section were honed after assembly. All other pipe joints were made in such a way as to ensure no wall discontinuities occurred along the length of the pipe.

The test section was provided with sets of static pressure holes at various axial locations. All holes were opened out in the boss to a connexion diameter equal to

twice the hole diameter, the length of hole being varied between tests to give the various length/diameter ratios. A Chattock gauge was employed to measure the small pressure differences, and the connexions to this gauge were made by rubber tubing of diameter equal to twice the hole diameter and length equal to 240 times the hole diameter.

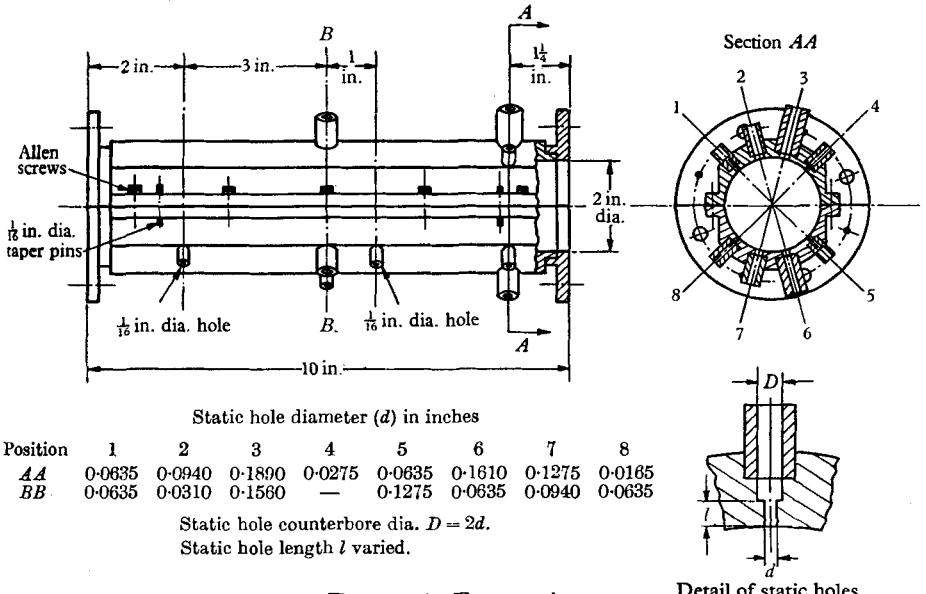

Static hole diameter (d) in inches

Position	1	2	3	4	5	6	7	8
AA	0·0635	0·0940	0·1890	0·0275	0·0635	0·1610	0·1275	0·0165
BB	0·0635	0·0310	0·1560	—	0·1275	0·0635	0·0940	0·0635

Static hole counterbore dia. $D = 2d$.
Static hole length l varied.

FIGURE 4. Test section.

7. Procedure

An attempt was made initially to use insert plugs located in a boss brazed on to the 6 ft. pipe section near the downstream flange, but it proved extremely difficult to hone the plug flush with the pipe wall, and the errors due to a protruding or recessed plug were of the same order as the errors due to hole size. The special test section was then machined and, in the first series of tests, was honed after drilling the holes. The test section was then split, and the appropriate drill shank inserted into each hole from the inside wall position to remove the internal burrs. The holes were then inspected for cleanliness and size using a traversing microscope. Honing and visual inspection were repeated until all the holes appeared to be free from burrs. These preliminary results were reported (Shaw 1958), but subsequent tests suggested that the sharp-edged form of the hole was destroyed by repeated honing. A Talysurf surface measuring instrument was then used to check the wall profile immediately before and after each hole, and this showed that the repeated honing had slightly rounded the edge of the holes, the effect being most marked with the larger holes. Since Rayle had shown that a radius tends to increase the positive error, it was apparent that new tests were necessary and that even greater care would be required in preparing the holes.

A new set of holes was located at section *AA* (figure 4), two reference holes 0·0635 in. diameter being provided. In this instance the test section was carefully honed before the holes were drilled, until the surface roughness indicated by the Talysurf instrument was less than 50 micro-inches. The holes were then drilled and

the burrs removed by careful hand polishing with fine grade emery paper wrapped round a semi-cylindrical wooden block, the surface finish and edge form being repeatedly checked on the Talysurf instrument until all burrs were removed. Internal burrs were removed using the drill shank and brass polish. Typical

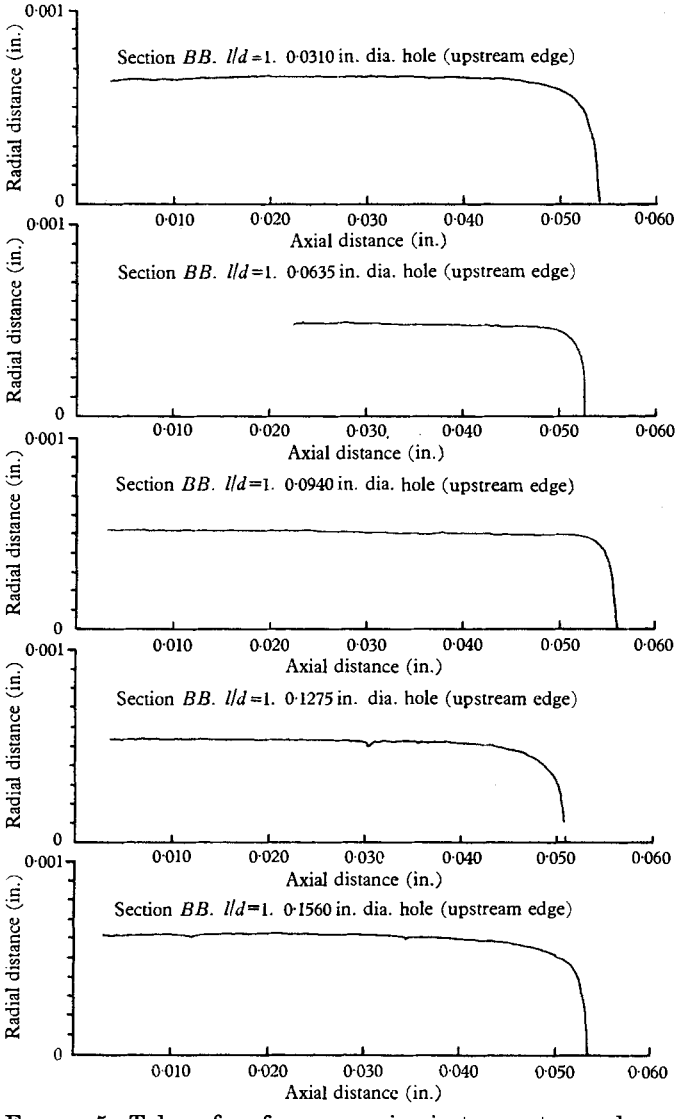

FIGURE 5. Talysurf surface measuring instrument records.

Talysurf records are shown in figure 5; the apparent inclination of the holes is due to the form of the Talysurf stylus. The length of the holes was reduced between tests using end mills of appropriate diameter to give l/d ratios of 6, 4, 2, 1 and 0·5, care being taken with the smaller holes to ensure that the inside wall of the pipe was not deformed.

The experiments were repeated for length/diameter ratios of 2, 1, and 0·5 using a further set of holes located at section BB (figure 4), the previous holes having

been plugged and the test section honed. In this case two additional precautions were taken. First, the dimensions of the pipe bore were checked using a Mercer cylinder gauge to ensure freedom from taper and ovality. These checks indicated that the maximum taper was 0·0003 in. per in. at section *BB* and that the maximum ovality was 0·0013 in. Second, in order to facilitate the drilling and end milling of the various holes, semi-cylindrical blocks were made to reinforce the pipe wall during these operations.

In the initial tests a null-reading inclined-tube type of micromanometer was used, but the results suggested that different viscous damping effects were produced by the asymmetry of the limbs. The Chattock gauge was therefore used because of its symmetry, but the dimensions of the manometer connexions were taken proportional to the hole size to preserve dimensional similarity up to the manometer. A further inconsistency in the results persisted at low velocities where the errors appeared to be comparatively large. Since this was thought to be due to some spurious effect originating at the three-stage blower, which was severely throttled at low flows, some of the later tests were carried out using the small single-stage blower. This eliminated the discrepancies.

For each test hole, readings of pressure error, relative to a reference hole, were recorded against the dynamic pressure at the $\frac{3}{4}$-radius position. The duplicate reference holes were used to assess the pressure difference between two nominally similar holes, and in general these differences were found to be small. At the maximum velocity the average difference was 0·007 in. of water (i.e. the absolute pressure error for the 0·0635 in. diameter reference hole, when $l/d > 1{\cdot}5$, is $0{\cdot}0360 \pm 0{\cdot}0035$ in. of water). The maximum difference between reference holes was 0·013 in. of water. Oscillations of the Chattock gauge bubble made accurate readings difficult at some velocities, the maximum bubble fluctuation being equivalent to about $\pm 0{\cdot}005$ in. of water. All observed relative errors were corrected to errors relative to the mean of the two reference holes.

On several occasions during the tests, readings were taken of pressure at the test section and also of the pressure drop over a 4 ft. length of test section. The mean velocity of flow was calculated from the observed dynamic pressure at the $\frac{3}{4}$-radius position, assuming the flow to be incompressible. The flow meter was calibrated initially by traversing one of the four Pitot tubes. The wall shear stress was calculated from the observed pressure drop at the test section, account being taken of the fluid acceleration due to compressibility, and the resistance coefficient $\gamma = \tau_0/\frac{1}{2}\rho u_m^2$ was plotted logarithmically against the pipe Reynolds number $D_p u_m/\nu$, where u_m is the mean flow velocity. These results were found to agree with Nikuradse's results for turbulent flow in a smooth pipe.

The results for length/diameter ratios between 1·5 and 6 were found to be the same, within the limits of experimental accuracy, and were therefore plotted on the one graph. After cross-plotting, graphs were drawn showing the pressure error, relative to the 0·0635 in. diameter reference holes, against diameter of hole for various mean velocities and length/diameter ratios (e.g. figure 6), and these curves were extrapolated to zero hole diameter to obtain absolute pressure errors. The extrapolations of these curves to zero hole diameter were made to fulfil two requirements, namely (1) that the curves pass as closely as possible

through the points obtained for small diameter holes; and (2) that the intercepts (at $d = 0$) are such that the absolute pressure errors, thereby obtained, give results which are consistent with the requirement, from similarity considerations, that the dimensionless pressure error is a function only of the Reynolds number $(d/\nu)\sqrt{(\tau_0/\rho)}$. Graphs of dimensionless pressure error against Reynolds number for various length/diameter ratios are shown in figures 7, 8 and 9.

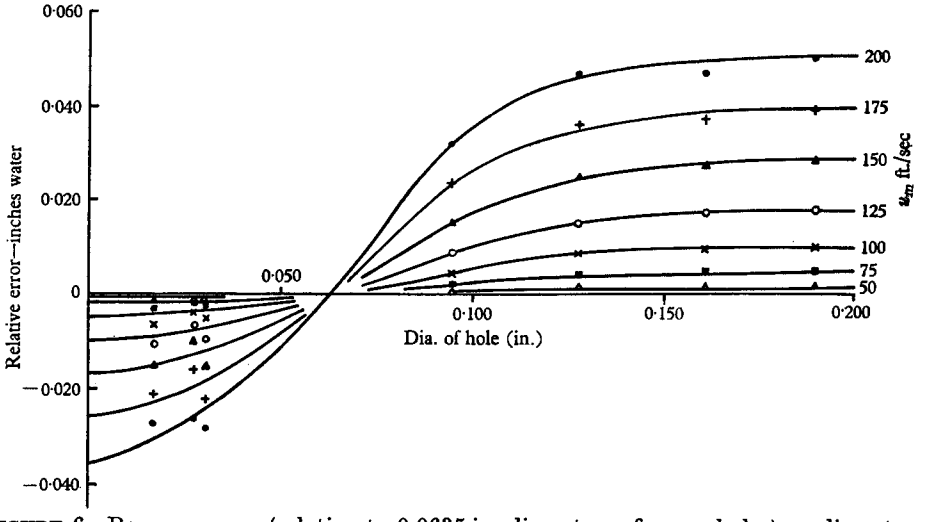

FIGURE 6. Pressure error (relative to 0·0635 in. diameter reference holes) *vs* diameter of hole for various mean velocities: l/d ratios 1·5 to 6.

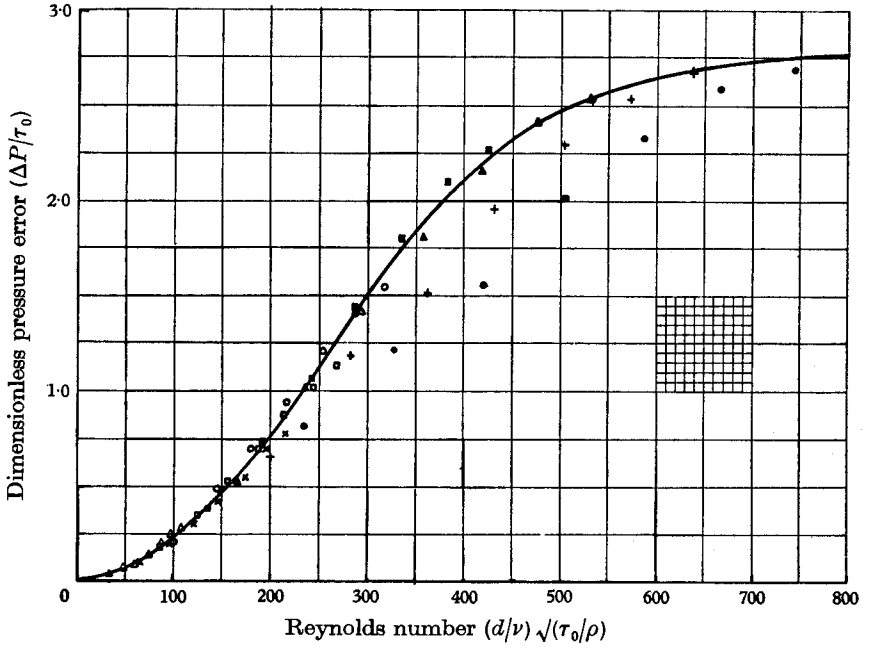

FIGURE 7. Dimensionless pressure error against Reynolds number for l/d ratios 1·5 to 6. Hole diameter (in.): ●, 0·175; +, 0·150; ▲, 0·125; ■, 0·100; ○, 0·075; □, 0·0635; ×, 0·050; △, 0·025.

Finally, four 0·0635 in. diameter holes with length/diameter ratios of 4 were drilled at a new axial location to assess the pressure error due to burrs projecting into the pipe. To obtained a variety of burrs, the holes were drilled with the semi-cylindrical support blocks in place, with the same drill speed, but with different

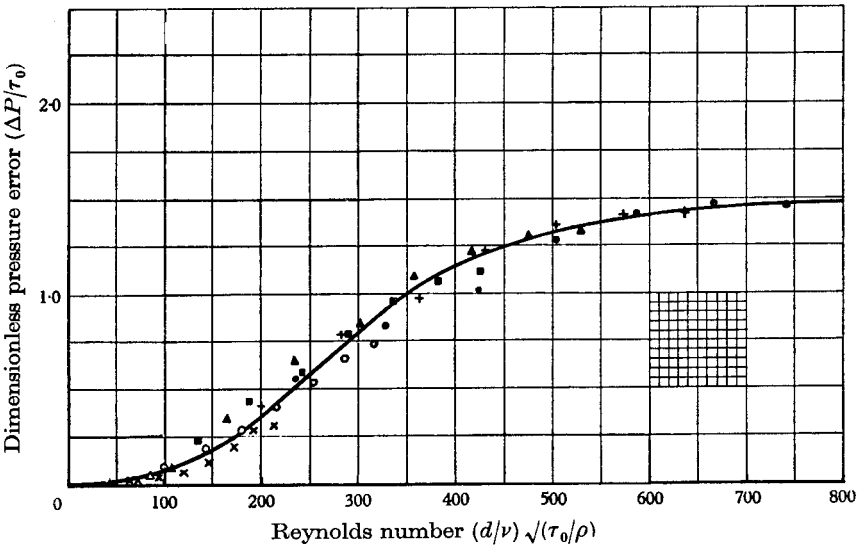

FIGURE 8. Dimensionless pressure error against Reynolds number for l/d ratio of 1. Hole diameter (in.): ●, 0·175; +, 0·150; ▲, 0·125; ■, 0·100; ○, 0·075; ×, 0·050; △, 0·025.

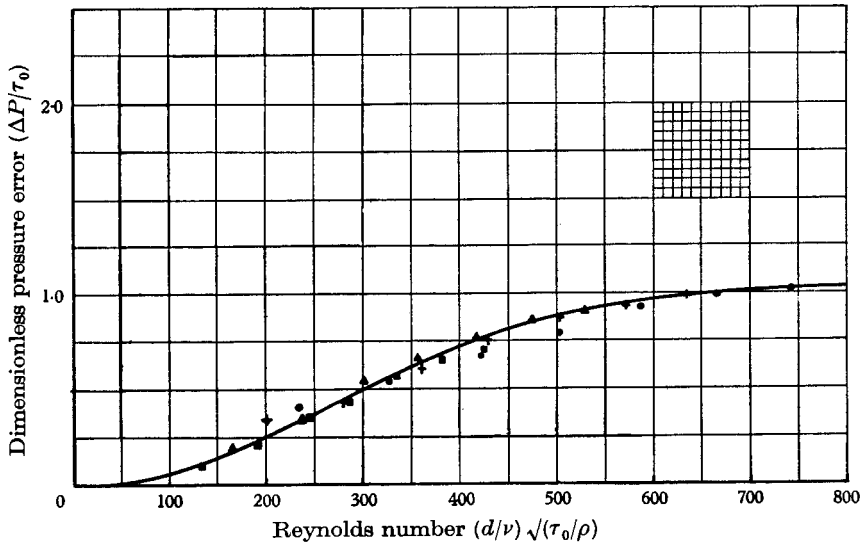

FIGURE 9. Dimensionless pressure error against Reynolds number for l/d ratio of 0·5. Hole diameter (in.): ●, 0·175; +, 0·150; ▲, 0·125; ■, 0·100.

feed rates; larger burrs being produced by higher feed rates. The burrs produced were measured on the Talysurf instrument and found to be 0·0003, 0·0004, 0·0017 and 0·0022 in. in height. The hole with the 0·0003 in. burr was then polished by hand until the burr was removed. A set of readings was then obtained

for the pressure error of the holes with drill burrs relative to this square edge hole for various mean velocities. The burrs were then reduced by hand polishing to 0·0001, 0·0004 and 0·0009 in. height, respectively, and the procedure repeated.

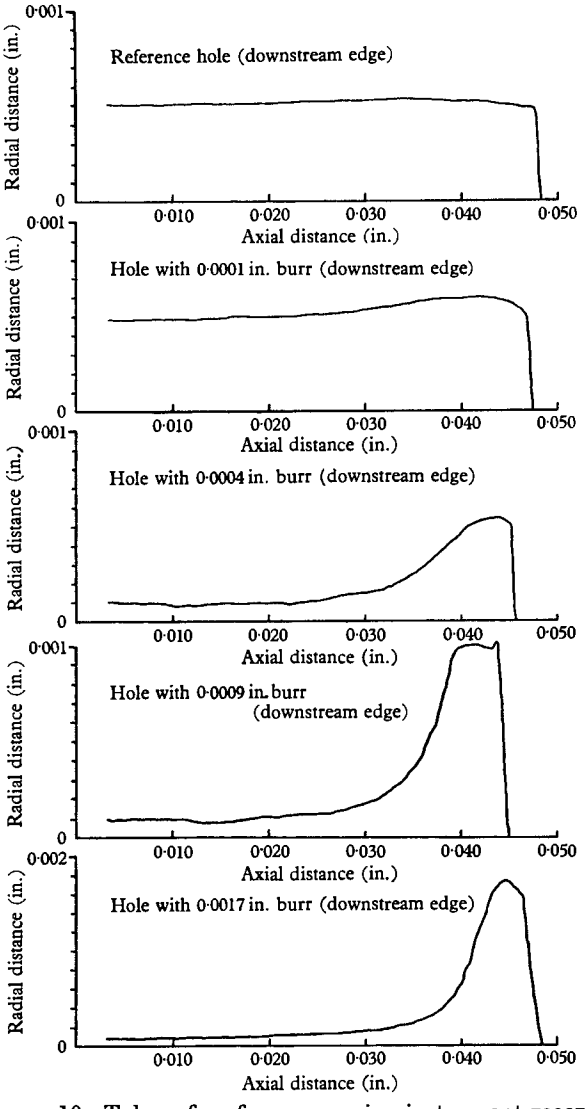

FIGURE 10. Talysurf surface measuring instrument records.

Talysurf records showing the shape of the burrs are shown in figure 10, and the results are plotted in dimensionless form in figure 11, together with the hole size error curve which is replotted on this curve for comparison purposes.

8. Discussion of results and comparison with results of other workers

The dimensionless curves of $\Delta P/\tau_0$ against $(d/\nu)\sqrt{(\tau_0/\rho)}$ (figures 7–9) show the form which was predicted by the dimensional analysis and the physical considerations. For $l/d > 1{\cdot}5$, the error is independent of the l/d ratio (figure 7), but

for $l/d = 1{\cdot}0$ (figure 8) and $l/d = 0{\cdot}5$ (figure 9) there is a progressive reduction in the error.

Inspection of figure 7 shows that the points for $d = 0{\cdot}175$ in. lie below the general curve. This might suggest that the hole diameter d is then sufficiently large compared with the pipe diameter D_p for the dimensionless group D_p/d to be significant. However, figures 8 and 9, for length/diameter ratios of 1 and 0·5, respectively, do not exhibit the same behaviour. A study of figure 6 indicates that if the measured relative error for the 0·1275 in. diameter holes is slightly excessive,

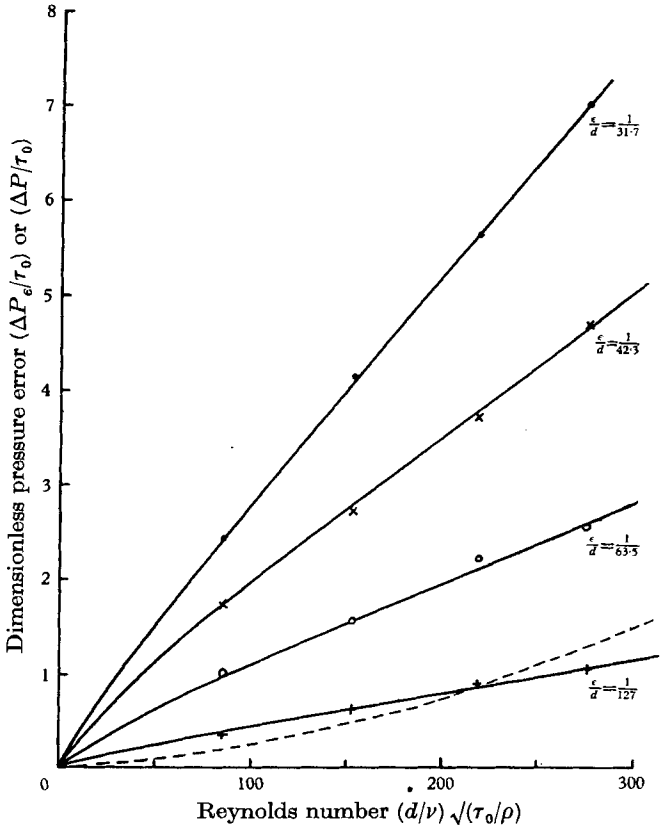

FIGURE 11. Dimensionless pressure error against Reynolds number for 0·0635 in. diameter holes with varying heights of radial burr: l/d ratio 4. —, $\Delta P_e/\tau_0$; – – –, $\Delta P/\tau_0$.

then the curves for each mean velocity would not tend to flatten at the larger hole diameters as much as is shown, and the points on figure 7 would then lie more nearly on a unique curve. It would therefore appear that the dimensionless group D_p/d is not significant for values greater than 10. Experiments with very large holes would be necessary to establish the onset of a D_p/d effect.

Figure 11 shows the effect of burrs formed in a natural manner during the drilling of the hole. For comparison, the hole-size error of a well-finished hole is shown, and it is immediately apparent that the effect of burrs is very significant. Similarly, specks of dust may have an important effect. From a practical standpoint, the smallest hole may not necessarily have the least error, since for a given

height of burr or speck of dust the effect will be larger for the small hole than for the larger one, and may well outweigh the error due to hole size.

Although no evidence of negative errors was obtained in the present experiments it is believed that such errors could be produced by holes of small length/diameter ratio which open out to very large diameters.

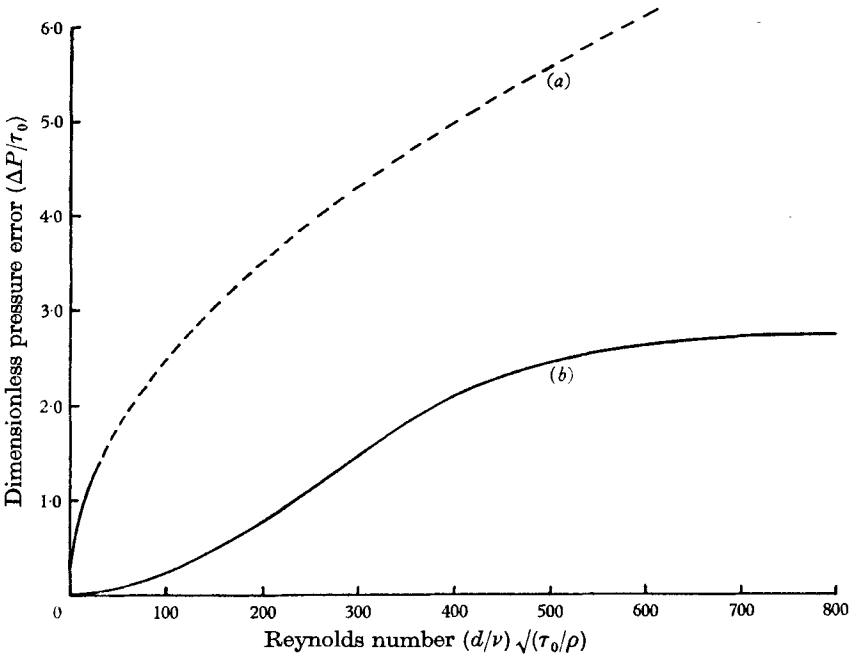

FIGURE 12. Dimensionless pressure error against Reynolds number for l/d ratio 1·5. Comparison with Ray's results (extrapolated for $R > 31$). (*a*) Ray's results for $l/d = 1{\cdot}5$, connexion diameter $< d$. (*b*) Present experimental results for $l/d = 1{\cdot}5$, connexion diameter $= 2d$.

Figure 12, showing Ray's results (extrapolated for $R > 31$) indicates that the dimensionless pressure errors in his case are considerably greater than the values found in this series of experiments. Some difference in the results can perhaps be attributed to the different connexion diameters employed, but the main source of difference occurs because of the method of extrapolation to zero hole diameter. In the first instance, Ray did not experiment with holes smaller than 0·039 in. diameter, and secondly, the intercepts for $d = 0$ were not selected in the way described above. Ray's correlation was carried out by assuming that the dimensionless error was proportional to R^{-n} (where $n > 0$) which was approximately true for his experimental points, but only for $d > 0{\cdot}039$ in.

Figure 13 gives a comparison with Rayle's results for incompressible flow. Rayle plotted a dimensionless pressure error $\Delta P/\frac{1}{2}\rho u_m^2$ against hole size for Mach numbers M of 0, 0·4 and 0·8. In his calculations for incompressible flow, the dimensionless errors for velocities varying from 22 to 31 ft./sec were averaged, Reynolds number effects being neglected. This gave a unique curve for $M = 0$. The variation of error with velocity was not clearly shown, because the velocity

range was limited, and an inclined manometer was employed to measure relative pressure errors.

Since it is the wall shear stress τ_0 which influences the error, it is desirable to plot the dimensionless pressure error as $\Delta P/\tau_0$. Therefore, taking Rayle's results for water flow in the case when the holes are located 27 diameters downstream of the nozzle and assuming the flow to be fully developed (Nikuradse suggests that for turbulent flow the 'length of transition' is 25–40 diameters), and reworking Rayle's results, using $\gamma = \tau_0/\frac{1}{2}\rho u_m^2$ from Nikuradse's curves for smooth pipes, we obtain the graph shown in figure 13. All the points are for relatively high mean

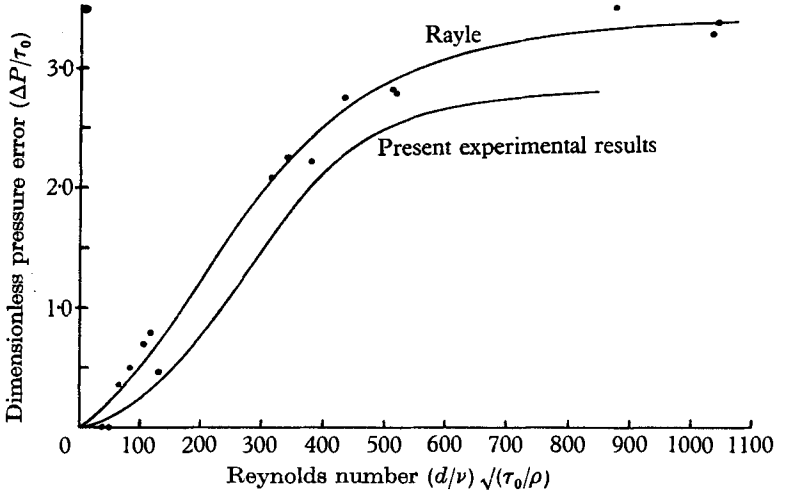

FIGURE 13. Dimensionless pressure error against Reynolds number for l/d ratio $> 1{\cdot}5$. Comparison with Rayle's results for incompressible flow.

velocities of flow, but the hole size varies from 0·006 to 0·125 in. diameter. If the flow in Rayle's experiments is not fully developed, then the correct

$$\tau_0 = \mu[du/dy]_{y=0}$$

will be greater than assumed, and this should reduce Rayle's $\Delta P/\tau_0$ to give even closer agreement than is indicated in figure 13.

9. Conclusions

For static pressure holes which are normal to the pipe wall, square-edged, and of length/diameter ratio between 0·5 and 6, with manometer connexion diameters twice the hole diameter, the pressure error is positive in turbulent flow and is a function of the Reynolds number $(d/\nu)/\sqrt{(\tau_0/\rho)}$ only, as shown in figures 7 to 9, for Reynolds numbers up to 800. The dimensionless error tends to zero for small Reynolds numbers, but increases progressively more rapidly with Reynolds number up to about 300, and then progressively less rapidly up to Reynolds number of 800, when the rate of increase is quite small. The error is only influenced by the length/diameter ratio of the hole for values of this ratio below 1·5, and is then found to be smaller.

For a smooth pipe with incompressible turbulent flow and a static pressure hole diameter one-tenth of the pipe diameter, the static pressure error reaches about 1 % of the mean dynamic pressure at a pipe Reynolds number of 2×10^5.

With a $\frac{1}{16}$ in. diameter hole of length/diameter ratio 4, the error due to a drill burr, which projects into the main stream, is approximately equal to the error due to hole size for a burr height ϵ of 0·0005 in. ($\epsilon/d = 1/127$), and is approximately seven times the error due to hole size for a burr height of 0·0020 in. ($\epsilon/d = 1/31{\cdot}7$), see figure 11.

The author wishes to thank Prof. J. H. Preston for permission to use the facilities of the Department of Fluid Mechanics and to acknowledge the assistance given by him during frequent discussions on this project.

REFERENCES

ALLEN, C. M. & HOOPER, L. J. 1932 Piezometer investigations. *Trans. A.S.M.E.* **54**, HYD 54–1.

FUHRMANN, G. 1912 Theoretische und Experimentelle Untersuchungen an Ballonmodellen. Dissertation, Göttingen.

MYADZU, A. 1936 Influence of type and dimensions of pressure hole on the recorded static pressure. *Ingen.-Arch.* **7**, 35.

PRESTON, J. H. 1950 The $\frac{3}{4}$ radius Pitot tube flow meter. *Engineer*, 27 October, p. 400.

PRESTON, J. H. 1958 The minimum Reynolds number for a turbulent boundary layer and the selection of a transition device. *J. Fluid Mech.* **3**, 373.

RAY, A. K. 1956 On the effect of orifice size on static pressure reading at different Reynolds numbers. *Ingen.-Arch.* **24** (3), 171. Translation in *A.R.C. Rep.* no. T.P. 498.

RAYLE, R. E. Jr. 1949 An investigation of the influence of orifice geometry on static pressure measurements. M.S. Thesis, M.I.T.

SHAW, R. 1958 The measurement of static pressure. *Report Advisory Group for Aeronautical Research and Development*, no. 163, p. 1.

THOM, A. & APELT, C. J. 1957 The pressure in a two-dimensional static hole at low Reynolds numbers. *A.R.C. Rep.* R. & M. no. 3090.